

Selected Papers

Enhanced Near-Infrared Luminescence of Yb(III) Complexes with Phosphine Oxide and Hexafluoroacetylacetonate Ligands

Shin-ichiro Kishimoto,[1] Tetsuya Nakagawa,[2,3] Tsuyoshi Kawai,[4] and Yasuchika Hasegawa*[1]

[1]Graduate School of Engineering, Hokkaido University, N13 W8, Kita-ku, Sapporo, Hokkaido 060-8628

[2]Center for Organic Photonics and Electronics Research (OPERA), Kyushu University, 744 Motooka, Nishi-ku, Fukuoka 819-0395

[3]Center for Future Chemistry, Kyushu University, 744 Motooka, Nishi-ku, Fukuoka 819-0395

[4]Graduate School of Materials Science, Nara Institute of Science and Technology, 8916-5 Takayama-cho, Ikoma, Nara 630-0192

Received August 26, 2010; E-mail: hasegaway@eng.hokudai.ac.jp

Near-infrared (NIR) luminescent Yb(III) complexes composed of low-vibrational frequency (LVF) fluorinated acetylacetonate and phosphine oxide ligands are reported. Their structures are determined using X-ray single-crystal analyses and categorized as eight-coordinated square antiprism. The radiative rate constants (k_r), the nonradiative rate constants (k_{nr}), and the 4f–4f emission quantum efficiency (Φ_{Em}) are estimated using their absorption spectra of magnetic dipole transition in Yb(III) complexes ($^2F_{5/2} \rightarrow {}^2F_{7/2}$) and the observed emission lifetimes. Characteristic NIR luminescence properties of Yb(III) complexes with LVF phosphine oxide and fluorinated acetylacetonate ligands are elucidated in terms of the radiative and nonradiative rate constants.

Near-infrared (NIR) luminescent lanthanide(III) complexes have been widely studied as luminescent molecules that can be used in fiber-optic telecommunication systems, lasers, electroluminescence devices, and biosensing applications.[1–4] NIR emissive Nd(III), Er(III), and Yb(III) complexes with various organic ligands have been reported during the last decade.[5] The NIR emission intensities of these lanthanide complexes are extremely weak. Radiationless transition via vibrational relaxation has been considered a dominant quenching process of the excited state of NIR emissive lanthanide complexes.[1] The vibrational relaxation of lanthanide complexes associate with the overtone of vibrational transition with high-frequency mode of ligand and/or solvent molecules. In order to enhance their NIR emission intensities and quantum efficiencies, it is necessary to suppress their radiationless transition via vibrational relaxation. To be concrete, chemical structures with high-frequency vibrational modes such as O–H, N–H, and C–H units should be removed from the vicinity of emissive lanthanide(III) centers.

We here focus on Yb(III) ion as a NIR luminescent center with relatively large emission intensity in the 4f–4f transition band, which is assigned to $^2F_{5/2} \rightarrow {}^2F_{7/2}$ (980 nm: magnetic dipole transition). The energy gap between $^2F_{7/2}$ and $^2F_{5/2}$ levels is found to be 10200 cm^{-1}, which is considerably larger than those of Nd(III) ion (5500 cm^{-1}) and Er(III) ion (6500 cm^{-1}).[1] According to energy-gap law,[6] lanthanide ions with larger energy gaps provide smaller nonradiative rate constants and higher emission quantum efficiency. Thus, Yb(III) ion with large energy gap could exhibit high NIR emission quantum efficiency in 4f–4f transition. The large energy gap of the Yb(III) center enables the introduction of common organic ligands with C–H bonds for the design of NIR luminescent Yb(III) complexes, although Nd(III) and Er(III) complexes should be coordinated with fully fluorinated ligands for NIR luminescence. We reported on the suppression of radiationless quenching in Eu(III) complexes with LVF hexafluoroacetylacetonate (hfa) and phosphine oxides with LVF coordination sites (triphenylphosphine oxide: tppo and 2,2′-bis(diphenylphosphoryl)biphenyl: biphepo).[7,8] Yb(III) complexes with tppo and biphepo ligands are expected to exhibit strong NIR luminescence. Pikramenou and co-workers have also suggested an advantage of LVF phosphine oxide ligands for luminescent lanthanide(III) complexes.[9] Yb(III) complex composed of LVF hfa and phosphine oxide ligands is thus expected to be a promising near-IR luminescent molecule with high emission quantum efficiency.

In the present study, we report on NIR luminescent Yb(III) complexes composed of LVF hfa and phosphine oxide ligands, $[Yb(hfa)_3(biphepo)]$ and $[Yb(hfa)_3(tppo)_2]$, and a Yb(III) complex containing acetylacetonate ligand with a phenyl group, 1-benzoyl-3,3,3-trifluoroacetonato: bta, $[Yb(bta)_3(biphepo)]$ (Figure 1). The coordination structures of the Yb(III) complexes are characterized using X-ray single-crystal analyses. The absorption spectra, the emission spectra, and the emission lifetimes of Yb(III) complexes are measured for estimations of the radiative rate constants (k_r), nonradiative (k_{nr})

Published on the web January 22, 2011; doi:10.1246/bcsj.20100241

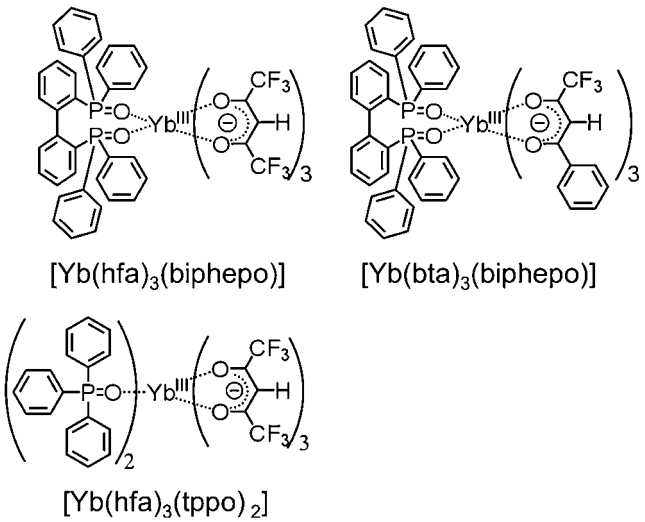

Figure 1. Chemical structures of [Yb(bta)$_3$(biphepo)], [Yb(hfa)$_3$(biphepo)], and [Yb(hfa)$_3$(tppo)$_2$].

rate constants, and the emission quantum efficiency (Φ_{Em}) in 4f–4f transition.[10,11] We also report that the estimated emission quantum efficiencies of prepared Yb(III) complexes are the highest in previously reported Yb(III) complexes with C–H vibrational frequency modes in their ligands. Characteristic NIR luminescence of Yb(III) complexes with LVF phosphine oxide and hfa ligands are demonstrated for the first time.

Experimental

Materials. Ytterbium(III) triflate hydrate (99.9%) and ytterbium(III) chloride hexahydrate were purchased from Wako Pure Chemical Industries Ltd. Methanol, dichloromethane, acetonitrile, and DMSO-d_6 were obtained from Nacalai Tesque, Inc. 1,1,1,5,5,5-Hexafluoro-2,4-pentanedione (hfa), 4,4,4-trifluoro-1-phenyl-1,3-butanedione (bta), 2,2′-bis(diphenylphosphoryl)biphenyl (biphepo), and triphenylphosphine oxide (tppo) were purchased from Tokyo Kasei Kogyo Co., Ltd. [Yb(hfa)$_3$(H$_2$O)$_2$] and [Yb(bta)$_3$(H$_2$O)$_2$] were prepared according to literature methods.[12,13] All other chemicals and solvents were reagent grade and were used without further purification.

Apparatus. IR spectra were recorded on a JASCO FT/IR-420 spectrometer. Elemental analyses were recorded on a Perkin-Elmer 2400IICHNS/O.

Preparation of Yb(III) Complexes. Preparation of [2,2′-Bis(diphenylphosphoryl)biphenyl]tris(hexafluoroacetylacetonato)ytterbium(III), [Yb(hfa)$_3$(biphepo)]: [Yb(hfa)$_3$(H$_2$O)$_2$] (1.8 g, 2.2 mmol) and 2,2′-bis(diphenylphosphoryl)-biphenyl (1.0 g, 1.8 mmol) were dissolved in methanol (60 mL) solution. The solution was then refluxed and stirred. After one day of stirring, the reaction mixture was evaporated. The pale yellow crystals of [Yb(hfa)$_3$(biphepo)] were obtained by recrystallization of the crude product with methanol (1.2 g, yield: 40%). IR (ATR): 3065, 1675, 1655, 1550, 1530, 1485, 1441, 1253, 1185, 1133, 1103 cm^{-1}. Anal. Calcd for $C_{51}H_{31}O_8F_{18}P_2Yb$: C, 45.42; H, 2.32; N, 0.00%, Found: C, 45.18; H, 2.19; N, 0.07%.

Preparation of Tris(1-benzoyl-3,3,3-trifluoroacetonato)-[2,2′-bis(diphenylphosphoryl)biphenyl]ytterbium(III), [Yb(bta)$_3$(biphepo)]: [Yb(bta)$_3$(H$_2$O)$_2$] (3.0 g, 3.5 mmol) and 2,2′-bis(diphenylphosphoryl)biphenyl (2.1 g, 3.9 mmol, 1.1 equiv) were dissolved in methanol (70 mL) solution. The solution was then refluxed with stirring for 1 h. White solid was deposited after 15 min of stirring. The reaction mixture was filtrated and the residue was recrystallized with MeOH/CH_2Cl_2 solution to afford the pale yellow crystals of [Yb(bta)$_3$-(biphepo)] (1.7 g, yield: 35%). IR (ATR): 3050, 2976, 2902, 2361, 1650, 1626, 1576, 1533, 1515, 1500, 1440, 1318, 1290, 1250, 1173, 1131, 1076 cm^{-1}. Anal. Calcd for $C_{67}H_{50}O_9F_9P_2Yb$ ([Yb(bta)$_3$(biphepo)]·MeOH): C, 57.27; H, 3.59; N, 0.00%. Found: C, 57.15; H, 3.54; N, 0.00%.

Preparation of Tris(hexafluoroacetylacetonato)bis(triphenylphosphoryl)ytterbium(III) [Yb(hfa)$_3$(tppo)$_2$]: [Yb(hfa)$_3$(H$_2$O)$_2$] (2.6 g, 3.1 mmol) and triphenylphosphine oxide (1.8 g, 6.5 mmol, 2.1 equiv) were dissolved in methanol (35 mL) solution. The solution was then refluxed and stirred. After 1 day of stirring, the reaction mixture was evaporated. The pale yellow crystals of [Yb(hfa)$_3$(tppo)$_2$] were obtained by recrystallization of the crude product with MeOH/MeCN (1:1) (2.7 g, yield: 64%). Anal. Calcd for $C_{51}H_{33}O_8F_{18}P_2Yb$: C, 45.35; H, 2.46; N, 0.00%. Found: C, 44.96; H, 2.35; N, 0.04%.

Optical Measurements. DMSO-d_6 solutions of [Yb(hfa)$_3$-(biphepo)], [Yb(bta)$_3$(biphepo)], and [Yb(hfa)$_3$(tppo)$_2$] (50, 13, and 50 mmol dm^{-3}, respectively) in quartz cells were degassed with bubbling N_2 for measurements of absorption spectra, emission spectra, and emission lifetimes. Absorption spectra of these Yb(III) complexes in DMSO-d_6 were measured on a JASCO V-550. In order to measure the emission spectra excited at the absorption band of 4f–4f transition, the solutions in quartz cells (optical path length, 10 mm) were excited at 940 nm ($^2F_{5/2}$–$^2F_{7/2}$) using a spectrometer (Jobin Yvon SPEX fluorolog-3 and photomultiplier (Hamamatsu R5509-72)) at room temperature. The spectra presented here were corrected for detector sensitivity and lamp intensity. Emission lifetimes of the Yb(III) complexes in DMSO-d_6 were measured with the third harmonics (355 nm) of a Q-swiched Nd:YAG laser (Spectra Physics, INDI-50, fwhm: 5 ns, $\lambda = 1064$ nm) and a photomultiplier (Hamamatsu photonics, R5108, response time 1.1 ns). The Nd:YAG laser response was monitored with a digital oscilloscope (Sony Tektronix, TDS3052, 500 MHz) synchronized to single-pulse excitation. Emission lifetimes were determined from the slope of logarithmic plots of decay profiles.

Crystallography. Pale-yellow single crystals of [Yb(hfa)$_3$-(biphepo)], [Yb(bta)$_3$(biphepo)], and [Yb(hfa)$_3$(tppo)$_2$] were mounted on a glass fiber with epoxy resin. X-ray diffraction intensities were collected with a Rigaku RAXIS RAPID (3 kW) imaging plate area detector with graphite monochromated Mo Kα radiation in the ω–2θ scanning mode at 193 ± 1 K. Hydrogen atoms were placed in calculated positions (C–H, 0.95 Å) and not refined. All calculations were performed with the Rigaku CrystalStructure 3.8.1 software.[14] The structure was solved by direct methods (SIR92[15]) and expanded using Fourier techniques (DIRDIF99[16]). The non-hydrogen atoms were refined anisotropically. Hydrogen atoms were refined using the riding model. The final cycle of full-matrix least-squares refinement (SHELXL97[17]) was based on observed reflections and variable parameters and converged (largest parameter shift was 0.00 times its esd) with unweighted and weighted agreement factors.

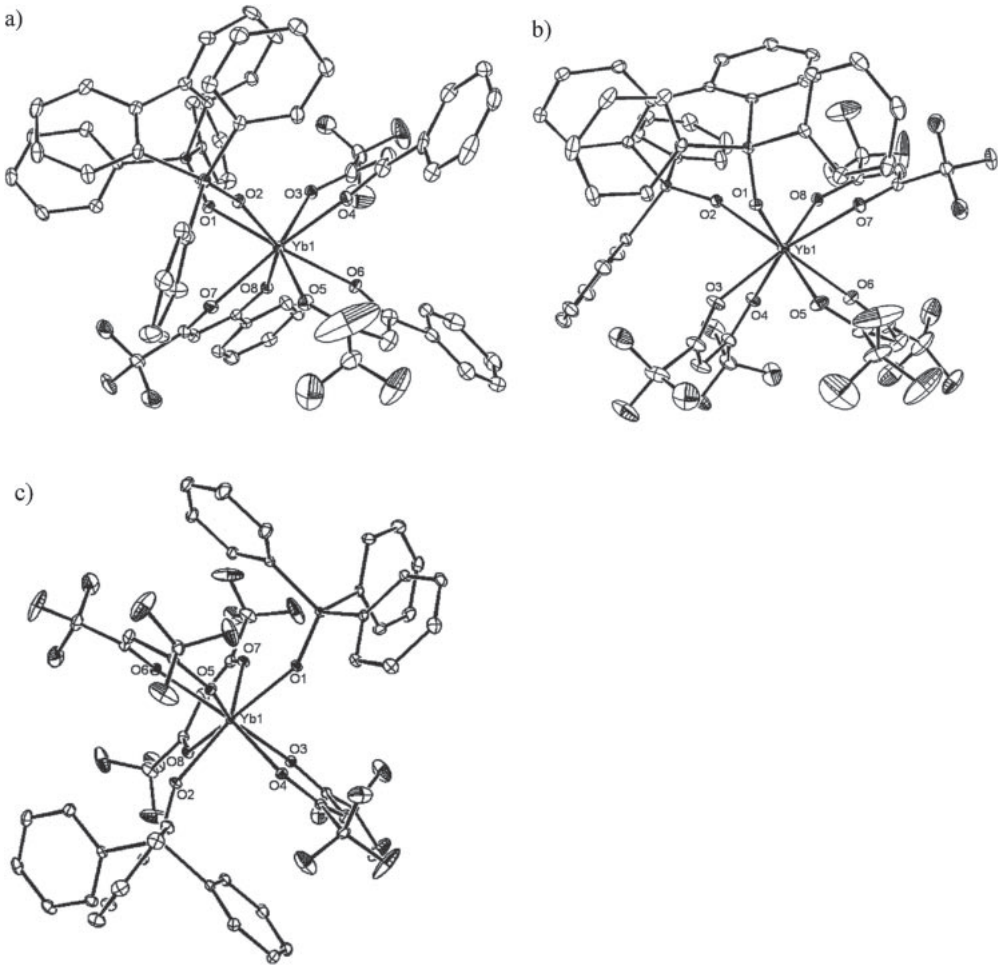

Figure 2. ORTEP views of a) [Yb(bta)$_3$(biphepo)], b) [Yb(hfa)$_3$(biphepo)], and c) [Yb(hfa)$_3$(tppo)$_2$].

Crystallographic data have been deposited with The Cambridge Crystallographic Data Centre: Deposition number CCDC-743762, -743763, and -799088 for [Yb(bta)$_3$(biphepo)], [Yb(hfa)$_3$(biphepo)], and [Yb(hfa)$_3$(tppo)$_2$]. Copies of the data can be obtained free of charge via www.ccdc.cam.ac.uk/data_request/cif (or from The Cambridge Crystallographic Data Centre, 12, Union Road, Cambridge, CB2 1EZ, UK; e-mail: data_request@ccdc.cam.ac.uk).

Results and Discussion

Coordination Structures. We carried out the X-ray single-crystal analyses of Yb(III) complexes for determination of their coordination structures. The ORTEP views and crystal data of [Yb(hfa)$_3$(biphepo)], [Yb(bta)$_3$(biphepo)], and [Yb(hfa)$_3$(tppo)$_2$] from X-ray single-crystal analyses are shown in Figure 2 and Table 1. The results of X-ray single-crystal analyses show that these Yb(III) complexes are composed of one bidentate or two monodentate phosphine oxide and three acetylacetonate ligands. Their structures are categorized as eight-coordinated square antiprism. Selected bond lengths between Yb(III) ion and oxygen atom in coordination sites are summarized in Table 2. The average distances between Yb(III) ion and oxygen atoms of phosphine oxide ligands in [Yb(bta)$_3$(biphepo)], [Yb(hfa)$_3$(biphepo)], and [Yb(hfa)$_3$(tppo)$_2$] were estimated to be 2.30, 2.25, and 2.22 Å, respectively. The larger distance in [Yb(bta)$_3$(biphepo)] might be caused by the three bta ligands containing the bulky phenyl group. On the other hand, the distances of these Yb(III) complexes are shorter than the distances between Yb(III) ion and oxygen atoms of acetylacetonate ligands in [Yb(bta)$_3$(biphepo)] (2.31 Å), [Yb(hfa)$_3$(biphepo)] (2.34 Å), and [Yb(hfa)$_3$(tppo)$_2$] (2.34 Å). These results indicate that the coordination ability of phosphine oxide is stronger than that of acetylacetonate ligands with trifluoromethyl groups. The strong coordination ability of phosphine oxide in Eu(III) complex have been reported.[7] The tight coordination of phosphine oxide molecules with low vibration (P=O: 1120 cm^{-1}) prevent coordination of high-vibrational molecules such as water. We consider that strong and tight coordination of phosphine oxides in Yb(III) complex might be held in organic liquid media.

Near-Infrared Absorption and Emission Properties. The absorption spectra of 4f–4f transitions in Yb(III) complexes and ytterbium(III) trifluoromethanesulfonate (Yb(OTf)$_3$) in DMSO-d_6 are shown in Figure 3. The absorption bands of [Yb(hfa)$_3$(biphepo)], [Yb(bta)$_3$(biphepo)], [Yb(hfa)$_3$(tppo)$_2$], and Yb(OTf)$_3$ were observed at 974 nm, and were assigned to $^2F_{7/2} \rightarrow {}^2F_{5/2}$ transition (magnetic dipole transition). Their absorption coefficients (ε) at 974 nm and the frequency-integrated absorption coefficients in the NIR region, $\int \varepsilon(\tilde{\nu})d\tilde{\nu}$, are shown in Table 3. The absorption coefficient and frequency-integrated

Table 1. Crystal Data Collection and Structure Refinement for [Yb(bta)$_3$(biphepo)], [Yb(hfa)$_3$(biphepo)], and [Yb(hfa)$_3$(tppo)$_2$]

	[Yb(bta)$_3$(biphepo)]	[Yb(hfa)$_3$(biphepo)]	[Yb(hfa)$_3$(tppo)$_2$]
Chemical formula	$C_{66}H_{46}F_9O_8P_2Yb$	$C_{51}H_{31}F_{18}O_8P_2Yb$	$C_{51}H_{33}F_{18}O_8P_2Yb$
Formula weight	1373.06	1348.76	1350.78
Crystal system	triclinic	monoclinic	monoclinic
Space group	$P\bar{1}$ (#2)	$P2_1/n$ (#14)	$P2_1/n$ (#14)
a/Å	12.1076(3)	13.1268 (2)	17.0948(4)
b/Å	12.9835(3)	31.8555(6)	15.3840(4)
c/Å	21.2565(5)	13.4771(3)	20.4822(5)
α/deg	86.0500(7)		
β/deg	81.2028(8)	110.6811(7)	93.9143(7)
γ/deg	64.9273(8)		
V/Å^3	2991.00(13)	5272.41(17)	5373.9(2)
Z	2	4	4
T/°C	−80	−80	−130
μ(Mo Kα)/cm^{-1}	17.004	19.505	19.138
No. of measured reflections	25277	42463	43310
No. of unique reflections	10932	9623	9788
R_{int}[a)]	0.0482	0.0303	0.0234
R_w[b)]	0.1648	0.0942	0.0556

a) $R_{int} = \Sigma||F_o| - |F_c||/\Sigma|F_o|$. b) $R_w = [\Sigma(w(F_o^2 - F_c^2)^2)/\Sigma w(F_o^2)^2]^{1/2}$.

Table 2. Selected Bond Lengths (Å) of Yb(III) Complexes

Bond	[Yb(bta)$_3$-(biphepo)]	[Yb(hfa)$_3$-(biphepo)]	[Yb(hfa)$_3$-(tppo)$_2$]
Yb–O1(P=O)	2.293(3)	2.245(2)	2.2241(17)
Yb–O2(P=O)	2.298(3)	2.259(2)	2.2238(17)
Average bond length	2.296	2.252	2.224
Yb–O3(C=O)	2.309(4)	2.321(2)	2.2937(17)
Yb–O4(C=O)	2.327(3)	2.330(2)	2.3557(16)
Yb–O5(C=O)	2.310(4)	2.348(2)	2.3819(16)
Yb–O6(C=O)	2.321(3)	2.329(2)	2.2869(16)
Yb–O7(C=O)	2.313(4)	2.327(2)	2.3491(18)
Yb–O8(C=O)	2.305(3)	2.370(2)	2.3555(16)
Average bond length	2.314	2.338	2.337

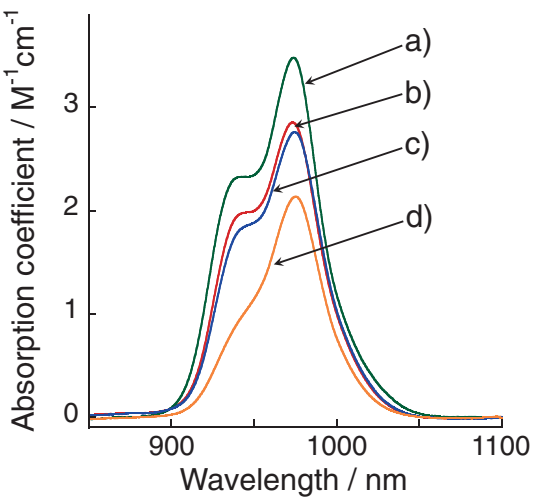

Figure 3. Absorption spectra of a) [Yb(bta)$_3$(biphepo)], b) [Yb(hfa)$_3$(biphepo)], c) [Yb(hfa)$_3$(tppo)$_2$], and d) Yb(OTf)$_3$ in DMSO-d_6 solutions.

Table 3. The Absorption Coefficients (ε) and Integral Absorption Spectra ($\int \varepsilon(\tilde{\nu})d\tilde{\nu}$) of $^2F_{5/2} \rightarrow {}^2F_{7/2}$ Transition of Yb(III) Complexes

Complex	λ^{Abs}_{Max} /nm	ε[b)] /M^{-1} cm^{-1}	$\int \varepsilon(\tilde{\nu})d\tilde{\nu}$ /M^{-1} cm^{-2}
[Yb(bta)$_3$(biphepo)]	974	3.2	2.4×10^3
[Yb(hfa)$_3$(biphepo)]	974	2.6	1.9×10^3
[Yb(hfa)$_3$(tppo)$_2$]	974	2.6	1.9×10^3
Yb(OTf)$_3$[a)]	974	2.1	1.2×10^3

a) Ytterbium(III) trifluoromethanesulfonate: Yb(CF$_3$SO$_3$)$_3$. b) The absorption coefficient is calculated on the basis of the molecular weight of anhydrate ytterbium(III) trifluoromethanesulfonate, 620.25.

absorption coefficient of [Yb(hfa)$_3$(biphepo)] were similar to those of [Yb(hfa)$_3$(tppo)$_2$]. We also noted that the absorption coefficient and frequency-integrated absorption coefficient of [Yb(bta)$_3$(biphepo)] are larger than those of [Yb(hfa)$_3$-(biphepo)] and [Yb(hfa)$_3$(tppo)$_2$]. The absorption coefficient and frequency-integrated absorption coefficient of Yb(OTf)$_3$ without organic ligand, Yb(OTf)$_3$, were found to be 2.1 and 1.2×10^3 M^{-1} cm^{-2}, respectively. We consider that organic ligands might affect the transition intensity of magnetic dipole transition in Yb(III) centers.

The emission spectra of [Yb(hfa)$_3$(biphepo)], [Yb(bta)$_3$-(biphepo)], and [Yb(hfa)$_3$(tppo)$_2$] shown in Figure 4 were measured under excitation at 940 nm ($^2F_{7/2} \rightarrow {}^2F_{5/2}$: excited at Yb(III) ion). The emission bands were also observed at 987 nm and assigned to the $^2F_{7/2} \rightarrow {}^2F_{5/2}$ magnetic dipole transition. We found that the spectral shape of [Yb(hfa)$_3$(biphepo)] was different from those of [Yb(bta)$_3$(biphepo)] and [Yb(hfa)$_3$-(tppo)$_2$] in DMSO-d_6. The characteristic spectral shapes of emission spectra result from the Stark splittings related to the coordination geometries of Yb(III) complexes. In DMSO-d_6, the coordination structure of [Yb(hfa)$_3$(biphepo)] might be

quite distinct from those of [Yb(bta)$_3$(biphepo)], [Yb(hfa)$_3$-(tppo)$_2$], and Yb(OTf)$_3$.

The time-resolved emission profiles of all Yb(III) complexes reveal single-exponential decays with lifetimes on the micro-second time scale as shown in Figure 5. The results in Figure 5 indicate single emissive components exist in the solution phase of each Yb(III) complex. The lifetimes were determined from the slopes of logarithmic plots of decay profiles. The observed lifetime of [Yb(bta)$_3$(biphepo)], [Yb(hfa)$_3$(biphepo)], and [Yb(hfa)$_3$(tppo)$_2$] were found to be 39, 49, and 55 μs, respectively (Table 4). Note that the emission lifetime of Yb(III) complex with bta ligands is smaller than those of Yb(III) complexes composed of hfa ligands. Generally, emission lifetime is influenced by radiative and nonradiative rate constants in the emission process. Large radiative rate constant and large nonradiative rate constant provide small emission lifetime. We expect that the radiative or nonradiative rate constants of Yb(III) complexes with bulky bta ligands, [Yb(bta)$_3$(biphepo)], will be different from those of Yb(III) complex with hfa ligand, [Yb(hfa)$_3$(biphepo)] and [Yb-(hfa)$_3$(tppo)$_2$].

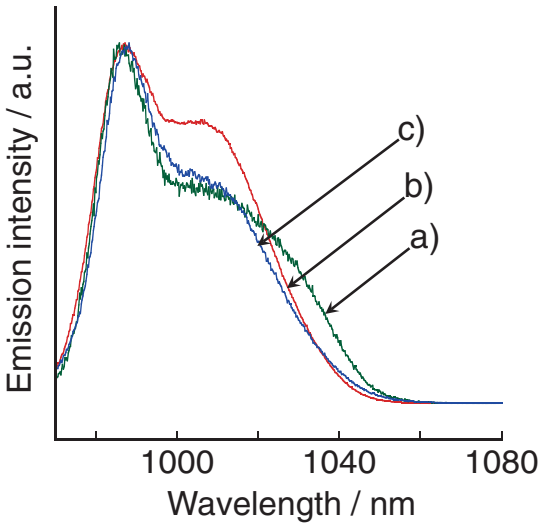

Figure 4. Emission spectra of a) [Yb(bta)$_3$(biphepo)], b) [Yb(hfa)$_3$(biphepo)], and c) [Yb(hfa)$_3$(tppo)$_2$] in DMSO-d_6 solutions (Ex. 940 nm).

Estimation of NIR Emission Quantum Efficiencies. In order to investigate photophysical processes of Yb(III) complexes, we estimated their radiative rate constants (k_r), nonradiative rate constants (k_{nr}), and the 4f–4f emission quantum efficiency (Φ_{Em}) using radiative lifetimes (τ_{rad}) and observed lifetimes (τ_{obs}).[10,11] The radiative lifetime is defined as an ideal emission lifetime without nonradiative processes. The radiative and observed lifetimes are expressed by,

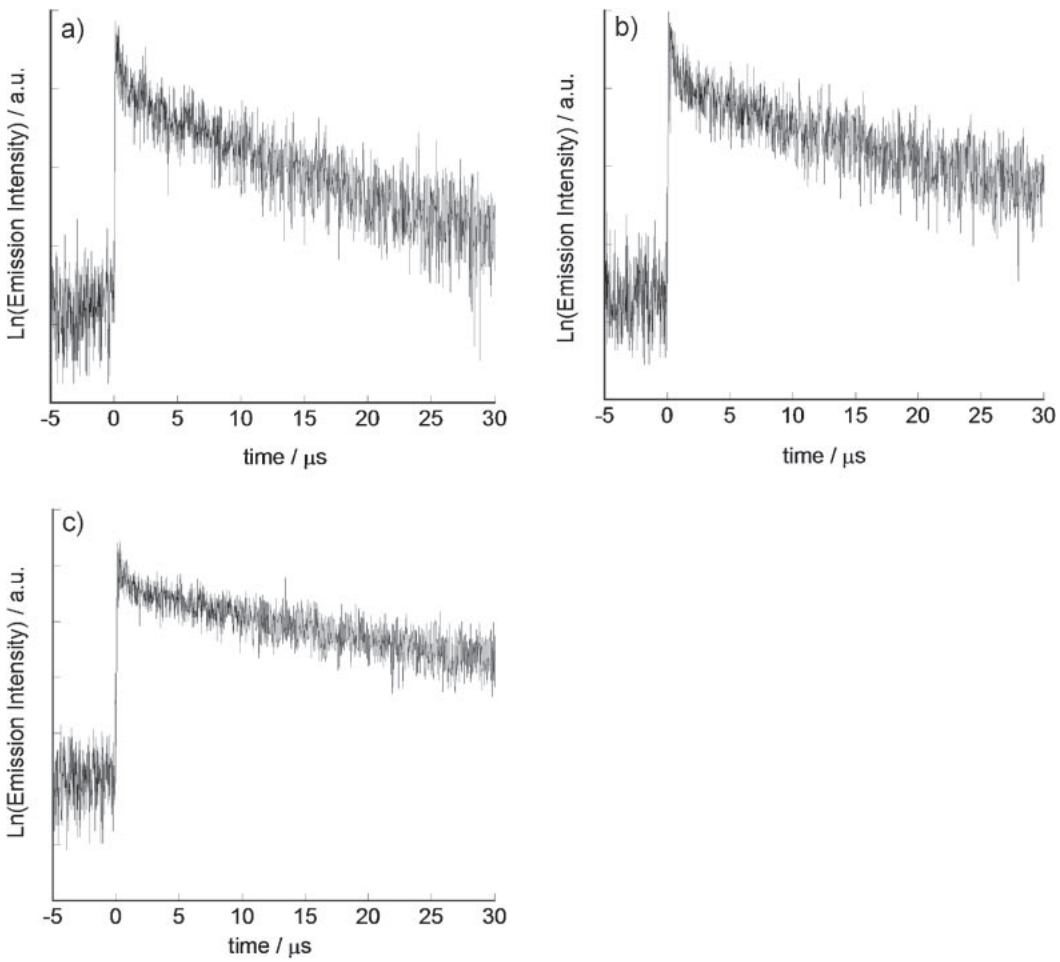

Figure 5. Emission decay profiles of a) [Yb(bta)$_3$(biphepo)], b) [Yb(hfa)$_3$(biphepo)], and c) [Yb(hfa)$_3$(tppo)$_2$] in DMSO-d_6 solutions.

Table 4. Radiative Rate Constants (k_r), Nonradiative Rate Constants (k_{nr}), and 4f–4f Emission Quantum Efficiency (Φ_{Em}) of Yb(III) Complexes

Complex	λ^{Abs}_{Max} /nm	λ^{Em}_{Max} /nm	τ_{obs} /μs	$\int \varepsilon(\tilde{\nu})d\tilde{\nu}$[a] /cm^{-2} M^{-1}	τ_{rad}[b] /μs	k_r[b] /10^3 s^{-1}	k_{nr}[c] /10^3 s^{-1}	Φ_{Em}[d] /%
[Yb(bta)$_3$(biphepo)]	974	986	39	2.4×10^3	4.7×10^2	2.1	24	8.0
[Yb(hfa)$_3$(biphepo)]	974	987	49	1.9×10^3	5.7×10^2	1.7	19	8.5
[Yb(hfa)$_3$(tppo)$_2$]	974	988	55	1.9×10^3	6.0×10^2	1.7	17	9.2
Yb(OTf)$_3$[e]	974	—	9.5[f]	1.2×10^3	1.2×10^3	0.82	110	0.77

a) Frequency-integrated absorption coefficients. b) Estimated from eq 3. c) Estimated from eq 5. d) Estimated from eq 6. e) Ytterbium(III) trifluoromethanesulfonate. f) Ref. 18.

$$\tau_{rad} = \frac{1}{k_r} \quad (1)$$

$$\tau_{obs} = \frac{1}{k_r + k_{nr}} \quad (2)$$

The radiative rate constants (k_r), nonradiative rate constants (k_{nr}), and the 4f–4f emission quantum efficiency (Φ_{Em}) of Yb(III) complexes are given by,

$$k_r = \frac{1}{\tau_{rad}} = 2300 \times \frac{8\pi c n^2 \tilde{\nu}_A{}^2}{N_A} \frac{g_l}{g_u} \int \varepsilon(\tilde{\nu})d\tilde{\nu} \quad (3)$$

$$\tilde{\nu}_{ul} = \frac{\int \tilde{\nu} \cdot \varepsilon(\tilde{\nu})d\tilde{\nu}}{\int \varepsilon(\tilde{\nu})d\tilde{\nu}} \quad (4)$$

$$k_{nr} = \frac{1}{\tau_{obs}} - \frac{1}{\tau_{rad}} \quad (5)$$

$$\Phi_{Em} = \frac{k_r}{k_r + k_{nr}} = \frac{\tau_{obs}}{\tau_{rad}} \quad (6)$$

where, c, $\tilde{\nu}$, n, N_A, $\varepsilon(\tilde{\nu})$, and g_l and g_u are the speed of light in vacuo, the frequency of the transition, the refractive index of the medium, Avogadro's constant, the absorption coefficient, and the degeneracies of the ground and excited states, respectively. The $\tilde{\nu}_A$ in eq 3 is a barycenter of the 4f–4f absorption transition. Calculated radiative lifetimes of [Yb(bta)$_3$(biphepo)], [Yb(hfa)$_3$(biphepo)], [Yb(hfa)$_3$(tppo)$_2$], and Yb(OTf)$_3$ were 467, 574, 607, and 1227 μs, respectively. Obtained k_r, k_{nr}, and Φ_{Em} of these Yb(III) complexes are shown in Table 4. The 4f–4f NIR emission quantum efficiency (Φ_{Em}) of [Yb(bta)$_3$(biphepo)], [Yb(hfa)$_3$(biphepo)], and [Yb(hfa)$_3$(tppo)$_2$] were estimated to be 8.0, 8.5, and 9.2%, respectively. These quantum efficiencies are the highest among those of previously reported Yb(III) complexes.[11]

We also found that the radiative rate constants (k_r) in the Yb(III) complexes were approximately ten times larger than those of reported Eu(III) complexes.[7,19] The larger radiative rate constants of Yb(III) complexes are caused by characteristics of spin allowed transition, fluorescence ($^2F_{5/2}$ ($S = 1/2$) → $^2F_{7/2}$ ($S = 1/2$), $\Delta S = 0$). On the other hand, the 4f–4f transitions of Eu(III) complexes are assigned to the spin-forbidden transitions, phosphorescence ($^5D_0$ ($S = 2$) → ^7F_J ($S = 3$), $\Delta S \neq 0$). We also observed that the k_r of [Yb(bta)$_3$(biphepo)] was larger than those of [Yb(hfa)$_3$(biphepo)] and [Yb(hfa)$_3$(tppo)$_2$]. The larger radiative rate constants of [Yb(bta)$_3$(biphepo)] might be due to distortion of the coordination structure composed of three bta ligand with bulky phenyl groups even under the 4f–4f transition of Yb(III) complexes. Demirkhanyan et al. have reported that the NIR emission from Yb(III) ion is composed of pure magnetic dipole transition and indirect electric dipole transition induced by Stark splitting of $^2F_{7/2}$ and $^2F_{5/2}$ state (IED transition).[20] The IED transition might provide large radiative rate constant of [Yb(bta)$_3$(biphepo)].

In contrast, we found that the nonradiative rate constant of [Yb(bta)$_3$(biphepo)] was larger than those of [Yb(hfa)$_3$(biphepo)] and [Yb(hfa)$_3$(tppo)$_2$]. The relatively larger nonradiative rate constant of [Yb(bta)$_3$(biphepo)] might be due to high-vibrational frequency modes of C–H bonds in bta ligands. These results suggest that the C–H bonds in acetylacetonate ligands in Yb(III) complexes lead to increase of nonradiative rate constants.[21] The replacement of C–H bonds with C–F or C–D bonds in low-vibrational acetylacetonate ligands is effective in suppression of radiationless transition via vibrational relaxation in Yb(III) complexs.[22]

Conclusion

We have demonstrated syntheses and photophysical properties of novel Yb(III) complexes with LVF phosphine oxide and hfa ligands. The 4f–4f NIR emission quantum efficiencies, radiative and nonradiative rate constants were estimated by the absorption spectra and observed emission lifetimes. The NIR emission quantum efficiencies of prepared Yb(III) complexes were the highest in previously reported Yb(III) complexes with organic ligands containing C–H bonds. We also found that the 4f–4f magnetic dipole transition of Yb(III) center was slightly affected by introduction of organic ligands. The replacement of C–H bond with C–F or C–D bonds in low-vibrational frequency acetylacetonate ligands is effective in suppression of radiationless transition via vibrational relaxation in Yb(III) complexs. These molecular designs of strong luminescent Yb(III) complex are expected to open up new fields in photonic molecular science.

We thank Dr. J. Yuasa (Graduate School of Materials Science, Nara Institute of Science and Technology) for technical support with the absorption spectra measurements. This work was supported partly by Grant-in-Aid for Scientific Research on the Priority Area "Strong Photon-Molecule Coupling Fields for Chemical Reactions," Scientific Research on Innovative Areas "Emergence in Chemistry" from the Ministry of Education, Culture, Sports, Science and Technology of Japan (MEXT), and Hokkaido Univ. Global COE Program "Catalysis as the Basis for Innovation in Materials Science."

References

1 a) D. Parker, *Chem. Soc. Rev.* **2004**, *33*, 156. b) K. Binnemans, *Chem. Rev.* **2007**, *107*, 2592. c) C. Piguet, J.-C. G. Bünzli, *Chem. Soc. Rev.* **1999**, *28*, 347. d) S. Claudel-Gillet, J. Steibel, N. Weibel, T. Chauvin, M. Port, I. Raynal, E. Toth, R. F. Ziessel, L. J. Charbonnière, *Eur. J. Inorg. Chem.* **2008**, 2856. e) H. Tsukube, S. Shinoda, *Chem. Rev.* **2002**, *102*, 2389. f) Y. Hasegawa, Y. Wada, S. Yanagida, *J. Photochem. Photobiol., C* **2004**, *5*, 183.

2 K. Kuriki, Y. Koike, Y. Okamoto, *Chem. Rev.* **2002**, *102*, 2347.

3 Y. Hasegawa, Y. Wada, S. Yanagida, H. Kawai, N. Yasuda, T. Nagamura, *Appl. Phys. Lett.* **2003**, *83*, 3599.

4 a) A. Ishii, S. Kishi, H. Ohtsu, T. Iimori, T. Nakabayashi, N. Ohta, N. Tamai, M. Melnik, M. Hasegawa, Y. Shigesato, *ChemPhysChem* **2007**, *8*, 1345. b) H. Akiba, J. Sumaoka, M. Komiyama, *ChemBioChem* **2009**, *10*, 1773.

5 a) J. Zhang, P. D. Badger, S. J. Geib, S. Petoud, *Angew. Chem., Int. Ed.* **2005**, *44*, 2508. b) N. M. Shavaleev, R. Scopelliti, F. Gumy, J.-C. G. Bünzli, *Eur. J. Inorg. Chem.* **2008**, 1523. c) G. A. Hebbink, L. Grave, L. A. Woldering, D. N. Reinhoudt, F. C. J. M. van Veggel, *J. Phys. Chem. A* **2003**, *107*, 2483. d) B. J. Coe, S. J. A. Pope, S. Faulkner, R. H. Laye, *Dalton Trans.* **2005**, 1482. e) G. Mancino, A. J. Ferguson, A. Beeby, N. J. Long, T. S. Jones, *J. Am. Chem. Soc.* **2005**, *127*, 524.

6 G. Stein, E. Würzberg, *J. Chem. Phys.* **1975**, *62*, 208.

7 Y. Hasegawa, M. Yamamuro, Y. Wada, N. Kanehisa, Y. Kai, S. Yanagida, *J. Phys. Chem. A* **2003**, *107*, 1697.

8 K. Nakamura, Y. Hasegawa, H. Kawai, N. Yasuda, N. Kanehisa, Y. Kai, T. Nagamura, S. Yanagida, Y. Wada, *J. Phys. Chem. A* **2007**, *111*, 3029.

9 P. B. Glover, A. P. Bassett, P. Nockemann, B. M. Kariuki, R. V. Deun, Z. Pikramenou, *Chem.—Eur. J.* **2007**, *13*, 6308.

10 M. H. V. Werts, R. T. F. Jukes, J. W. Verhoeven, *Phys. Chem. Chem. Phys.* **2002**, *4*, 1542.

11 N. M. Shavaleev, R. Scopelliti, F. Gumy, J.-C. G. Bünzli, *Inorg. Chem.* **2009**, *48*, 7937.

12 H.-B. Xu, L.-Y. Zhang, X.-M. Chen, X.-L. Li, Z.-N. Chen, *Cryst. Growth Des.* **2009**, *9*, 569.

13 A. I. Voloshin, N. M. Shavaleev, V. P. Kazakov, *J. Lumin.* **2000**, *91*, 49.

14 *CrystalStructure Ver.3.8.1 Software*, Rigaku Corporation, **2006**.

15 SIR92: A. Altomare, G. Cascarano, C. Giacovazzo, A. Guagliardi, M. C. Burla, G. Polidori, M. Camalli, *J. Appl. Crystallogr.* **1994**, *27*, 435.

16 P. T. Beurskens, G. Admiraal, G. Beurskens, W. P. Bosman, R. de Gelder, R. Israel, J. M. M. Smits, *DIRDIF-99 Program System, Technical Report of the Crystallography Laboratory*, University of Nijmegen, The Netherlands, **1999**.

17 G. M. Sheldrick, *SHELXL-97, Program for the Refinement of Crystal Structures*, University of Göttingen, Germany, **1997**.

18 A. Beeby, R. S. Dickins, S. Faulkner, D. Parker, J. A. G. Williams, *Chem. Commun.* **1997**, 1401.

19 K. Miyata, Y. Hasegawa, Y. Kuramochi, T. Nakagawa, T. Yokoo, T. Kawai, *Eur. J. Inorg. Chem.* **2009**, 4777.

20 a) G. G. Demirkhanyan, *Laser Phys.* **2006**, *16*, 1054. b) G. G. Demirkhanyan, V. G. Babajanyan, E. P. Kokanyan, R. B. Kostanyan, J. B. Gruber, D. K. Sardar, *Opt. Mater.* **2007**, *29*, 1107.

21 P. He, H. Wang, S. Liu, J. Shi, G. Wang, M. Gong, *J. Phys. Chem. A* **2009**, *113*, 12885.

22 G. A. Hebbink, D. N. Reinhoudt, F. C. J. M. van Veggel, *Eur. J. Org. Chem.* **2001**, 4101.